# Advanced partial discharge testing of 540V aeronautic motor fed by SiC inverter under altitude conditions

Thibaut Billard, Cédric Abadie, Bouazza Taghia

# Advanced Partial Discharge Testing of 540V Aeronautic Motors Fed by SiC Inverter under Altitude Conditions

**Thibaut BILLARD, Cedric Abadie, and Bouazza Taghia**
IRT Saint-Exupery

**CITATION:** BILLARD, T., Abadie, C., and Taghia, B., "Advanced Partial Discharge Testing of 540V Aeronautic Motors Fed by SiC Inverter under Altitude Conditions," SAE Technical Paper 2017-01-2029, 2017, doi:10.4271/2017-01-2029.

## Abstract

The present paper reports non-electrically intrusive partial discharge investigations on aeronautic and electric vehicle motors fed by SiC inverter drive under variable environmental conditions. A representative test procedure and experimental set-up based on operating aeronautic conditions are essential to ensure the accuracy and reliability of partial discharge test on aircraft systems to make informed decisions on insulation system design choice. The aim of this paper is to demonstrate the feasibility of partial discharge test of the insulation system on a different type of motor under such conditions, both electrically and environmentally.

To do so, the paper will start by detailing the innovative experimental set-up to be used in the study. It mainly consists in a high-voltage (1000V) inverter drive using SiC components to provide fast rise time surges. A vacuum chamber is used to simulate altitude while the association of non-intrusive sensors, analog filtering and wavelet based signal processing provided partial discharge detection.

Then, an analysis is carried out on several motors to find out which voltage magnitude trigger partial discharge events. The study helps to realize the benefits of using an inverter based test method to find the limits of the insulation system under various pressure and electrical conditions. It is shown that a representative insulation system performance picture could be drawn experimentally and used to enhance insulation design and manufacturing choices.

This paper will also review the ability of the non-intrusive test method and the associated numerical signal processing to detect partial discharge in a motor fed by fast-rise time surge and under different pressures. The paper concludes with an analysis of results and thoughts about future work regarding advanced test procedure.

## Introduction

### *Background*

Optimization of energy sources aboard aircraft and permanent improvements in more electric technologies are pushing the aeronautic industry to aim for the more electrical aircraft (MEA).

Indeed, electric energy offers numerous benefits in aircrafts. First, power generation, distribution and conversion are easier because being more accurate and flexible than pneumatic or hydraulic energy control. Then, significant mass reduction seems more likely to be achieved than with traditional hydraulic systems needing large, heavy and maintenance intensive distribution system.

But, this shift towards MEA is not without consequences on the electrical stress the insulation system has to withstand. Thus, with primary voltage increasing, power distribution architecture evolution and high power density power electronics, partial discharge (PD) is now a serious cause of concern for aircraft integrator, system designer and component manufacturer. Once PDs are occurring regularly, degradation of the insulation system until premature failure of the aircraft system is irremediable.

### *Scope and Goal of the Work*

This topic of interest has already been discussed by several key actors of the aerospace industry, research center such as US Air force laboratory or international academic actors. All acknowledge that PD risk in a harsh aeronautic environment where pressure, temperature and humidity variation, electrical stress created by inverter and harness length and weight increase. [1, 2, 3, 4]

Among key issues of aeronautic companies that has to be investigated at IRT Saint-Exupéry, the ability to accurately detect PD on different electric motors in an electrically non-intrusive way and under representative aeronautic environment when fed by a silicon carbide (SiC) inverter drive will be addressed in this paper and will be the main contribution.

Indeed, it has been recently demonstrated that on-line PD detection on electric motors fed by inverter drive proves to be possible using non-intrusive sensors. A broad range of operating electric motors have been tested on industrial test benches under nominal conditions to validate and define the limitations of the whole non-intrusive PD detection method [5]. Moreover, a previous analysis illustrated the gains of carrying out a detailed and progressive analysis of the insulation system both under AC and impulse voltage from twisted pair sample to a complete stator [6]. But, as a whole, a key link in the testing chain was still missing. So, in order to make one step further, a unique and new testing mean has been designed at IRT Saint-Exupéry and will be used in this paper. It is a highly customizable three phases SiC inverter drive with a high voltage DC bus of 1kV.

The aim of this experimental set-up is thus to help electric motor designer evaluate the quality of the insulation system under harsh electrical conditions before making the final test under nominal operating conditions. The three kind of PD tests conditions (simple off-line, inverter harsh off-line and nominal conditions on-line) are thus complementary and give the full picture of the insulation system.

## Outline

First, partial discharge key points and its consequences on insulation system will be recalled. In a second step, key features of more electrical aircraft will be recalled and how they relate to the innovative experimental set-up used here. Then, its main characteristics will be presented and an analysis is made regarding the relation between time, dV/dt and overvoltage.

The impact of a SiC inverter drive on the non-intrusive detection sensitivity will be evaluated. Comparison between analog filtering and wavelet numerical processing will be presented as a mean to double-check partial discharge inception (PDIV) values.

Then, details of the 3 stator will be presented and will be followed by tests results and analysis. Stator n°1 illustrates the potential consequences of undetected partial discharge on the insulation system and its consecutive failure. Stator n°2 illustrates the performance of the whole experimental set-up both at atmospheric and low pressure. Stator n°3 demonstrate how different winding configurations could be used to enhance PDIV for the same insulation system. Finally, a short discussion is followed by details of future work.

## Partial Discharge Basics

### *What is a Partial Discharge? IEEE Definition*

According to IEEE standard definition [7] a partial discharge is:

**An electrical discharge that only partially bridges the insulation between conductors. A transient gaseous ionization occurs in an insulation system when the electric stress exceeds a critical value, and this ionization produces partial discharges.**

Figure 1. Partial discharge at 100mbars between phase under AC 5kHz and opening time 30s [6]

### *Consequences of Partial Discharge*

Partial discharge events have been known and studied for more than a century, starting with Paschen, Peek and Townsend among others. Partial discharges are feared because they contribute to the degradation of the insulation system and lead to its premature failure [8] as will be shown in this paper.

### *Partial Discharge in More Electrical Aircraft*

With the recent increase in voltage from 115 V AC to 230 V AC or ±270 VDC on HVDC network, that risk has to be taken into account in designing equipment and in qualification process.

Moreover, it is known from Paschen curve that partial discharge risk is highly linked to pressure level. Since this variation is non-linear with pressure, it is assumed that no simple scale factor could be applied to predict partial discharge inception voltage from results at atmospheric pressure. Indeed, it is impossible to state *a priori* that the weakest insulation point test at atmospheric pressure is also the weakest insulation point at low pressure so that a scale factor is a sound hypothesis. It is thus mandatory to carry out test across the whole range of pressure.

### *Partial Discharge Inception Voltage*

According to IEEE Standard [7], PDIV is

**The lowest voltage at which continuous partial discharges (PDs) above some stated magnitude (which may define the limit of permissible background noise) occur as the applied voltage is increased. Many factors may influence the value of PDIV, including the rate at which the voltage is increased as well as the previous history of the voltage applied to the winding or component thereof**

PDIV could be expressed either at RMS or peak voltage depending on the applied voltage during test.

During partial discharge test of equipment, PDIV is usually a representation of the insulation system quality. In other words, it represents its ability to withstand a defined voltage level before partial discharge occurs.

It is thus of a critical importance to that tests are robust, easy to reproduce and relevant for the foreseen application. It is also important to have an accurate PDIV measurement method that could be applied indistinctly on all the aforementioned configuration. From simple material characterization test at atmospheric pressure, to an operating system in a low pressure environment.

Failure of reporting an equipment subject to partial discharge could have dramatic consequence on its reliability, leading to short-circuits creating electrical arcs. Safe level of target PDIV should be set in order to ensure equipment are PD free during operational life of the system.

## More Electrical Aircraft Paradigm

The MEA approach underlines the use of electrical system for non-propulsive application such as environmental control systems (ECS), electric driven hydraulic pump or flight control actuation. Other applications such as electrical taxiing or anti-icing are also considered for electrification. In other words, a more electrical aircraft has no on-engine hydraulic power generation and bleed air off-takes but more and more power electronics and electric motors.

### *Key Role of Highly Integrated Power Electronics*

A key enabler of such development is the breakthrough in high power density, high voltage and reliable silicon-based power semiconductor switching device such as insulated gate bipolar transistor (IGBT).

It is expected that state-of-the-art switching device such as Silicon Carbide (SiC) or Gallium Nitride (GaN) will dramatically improve inverter drive, converters, motor controller and other semiconductor based power systems power density, fulfilling at the same time mass reduction objective and electric power increase.

The evolution of power electronics towards fast switching in the more electrical aircraft with HV AC and HV DC network increased primary voltage is putting even more stress on motor insulation system [9, 10, 11, 12]

The combination of harness length, fast rise time is creation overvoltage at motor terminals and an uneven voltage distribution is found on coils increasing electrical stress on the turn-to-turn insulation system. The following experimental set-up aims to recreate such electrical stresses

## Experimental Set-Up

### *Power Supplies*

#### High Speed High Voltage Power Amplifier

Associated with a Tektronix AFG3022 dual channels arbitrary waveform generator, the Trek 10/40A-HS amplifier is able to deliver 10kV peak and a maximum of 40mA RMS current with a bandwidth of 23 kHz. This versatility allows different voltage waveforms to be tested such as AC at various frequency, square bipolar with adaptable duty cycle, frequency and other point-per-point signals.

#### High Voltage SiC Inverter Drive

An inverter drive has been designed at IRT Saint Exupéry to recreate a typical aeronautical electromechanical chain. For the DC bus voltage, two 15kW 500V ElektroAutomatic DC power supplies are in series with the mid-point grounded, the total DC bus voltage could remotely be varied from ± 10V to ± 500V.

The inverter drive consists in three 1700V SiC Cree power modules delivering fast rise times on each phase with driver boards accepting a switching frequency up to 20 kHz. Any PWM command made in a Matlab-Simulink model could be used to control the inverter drive thanks to the use of an OPAL-RT real time calculator. Switching frequency, carrier frequency and modulation factor could easily be modified. Command signals are transmitted using two optical fibers per phase (enable and command) allowing the use of the inverter as a half-bridge, full-bridge or three phase configurations as needed.

#### High Voltage Measurements

Voltage level are monitored using a Testec TT-SI 9010A (1/1000 ratio) active differential probe whose bandwidth is 70MHz.

### *Signal Acquisition*

#### Analog to Digital Conversion

Data are displayed and recorded using a Keysight DSOS204A oscilloscope with a sampling rate of 20GSa/s and numerical bandwidth of 2GHz. All PDIV measurements were made in peak detect mode with sampling frequency fixed at 5GS/s. If data need to be processed numerically, the high resolution mode (12 bits) is used instead of the peak detect mode at the higher sampling frequency available.

#### Analog High Pass-Filtering

When performing measurement using non-intrusive sensor, it is usual to connect high-pass analog filter before the oscilloscope be to remove noise coming from inverter drive switches or power amplifier. Typical cut-off frequency range from 25MHz to 200MHz have been used in the following experiments

#### Partial Discharge Sensors

Technological research at IRT Saint-Exupéry are focused on non-intrusive sensors. These sensors and associated method have already prove to be effective for detecting partial discharge on-line on both electric motor in automotive [2] and aeronautic test benches [5].

##### *Capacitive Sensor*

The non-intrusive sensor used to detect partial discharge is taking advantage of the capacitive effect. More details are provided on the sensor behavior in the next part. This sensor has already been used in numerous study, particularly [2] and [6].

### *Environmental Conditions*

All the tests have been carried out within a grounded vacuum chamber, acting as a faraday chamber, connected to a vacuum pump. The system is currently able to regulate pressure from atmospheric to 20mbars with an accuracy of +/- 5 mbars.

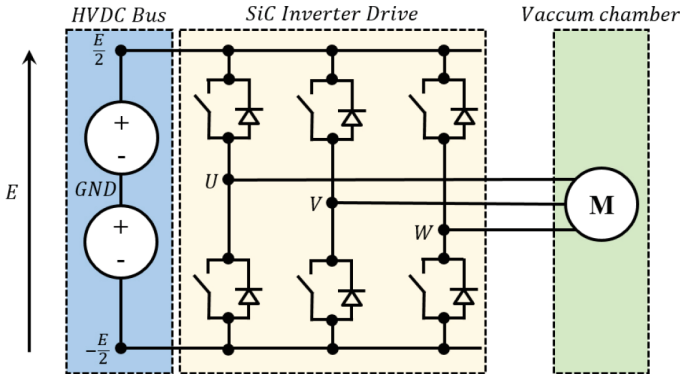


Figure 2. SiC inverter drive altitude experimental set-up

Table 1. Inverter drive operating point

| | |
|---|---|
| Switching frequency | 20 kHz |
| Carrier frequency | 500 Hz |
| DC Bus | 700V (±350V) |
| Modulation factor | 0.5 |
| Harness length | 1 m |

### *Rise Time and Overvoltage Measurement*

To briefly demonstrate the performance of the SiC inverter drive, a time dependent rise time and overvoltage analysis has been carried out while feeding a three phase electric. Measurements were performed directly at inverter output using a high voltage differential probe between the DC- and the output of the power module. Table 1 details the used operating point.

In IEC 60034-18-41 standard [13], stress magnitude categories are defined according to rise time and overvoltage value compared to nominal DC bus voltage. It is thus interesting to track the time dependent evolution of this parameters to check when the electrical stress is the most severe.

Typical SiC inverter behavior could be observed on both rise time and overvoltage which is both are current dependent. Although current was not monitored during measurement, the time dependency and periodicity could be observed on rise time which is maximum at current polarity reversal while minimum when current is at his highest value. On the contrary, overvoltage is maximum when current is at its maximum while overvoltage is minimum at current polarity reversal. As a result, the electrical stress created by the combination of dV/dt and overvoltage is time dependant.

These phenomena could be explained by the very nature of SiC switch, current magnitude, grid resistor and other power electronics characteristics. In essence, dV/dt is maximum for low current turn-on while overvoltage is generally maximum during turn-off [14]. This is shown on Fig.3 for falling edge in red.

On both rising edge and falling edge, the effect on switching on other phase could be observed by small perturbations on overvoltage.

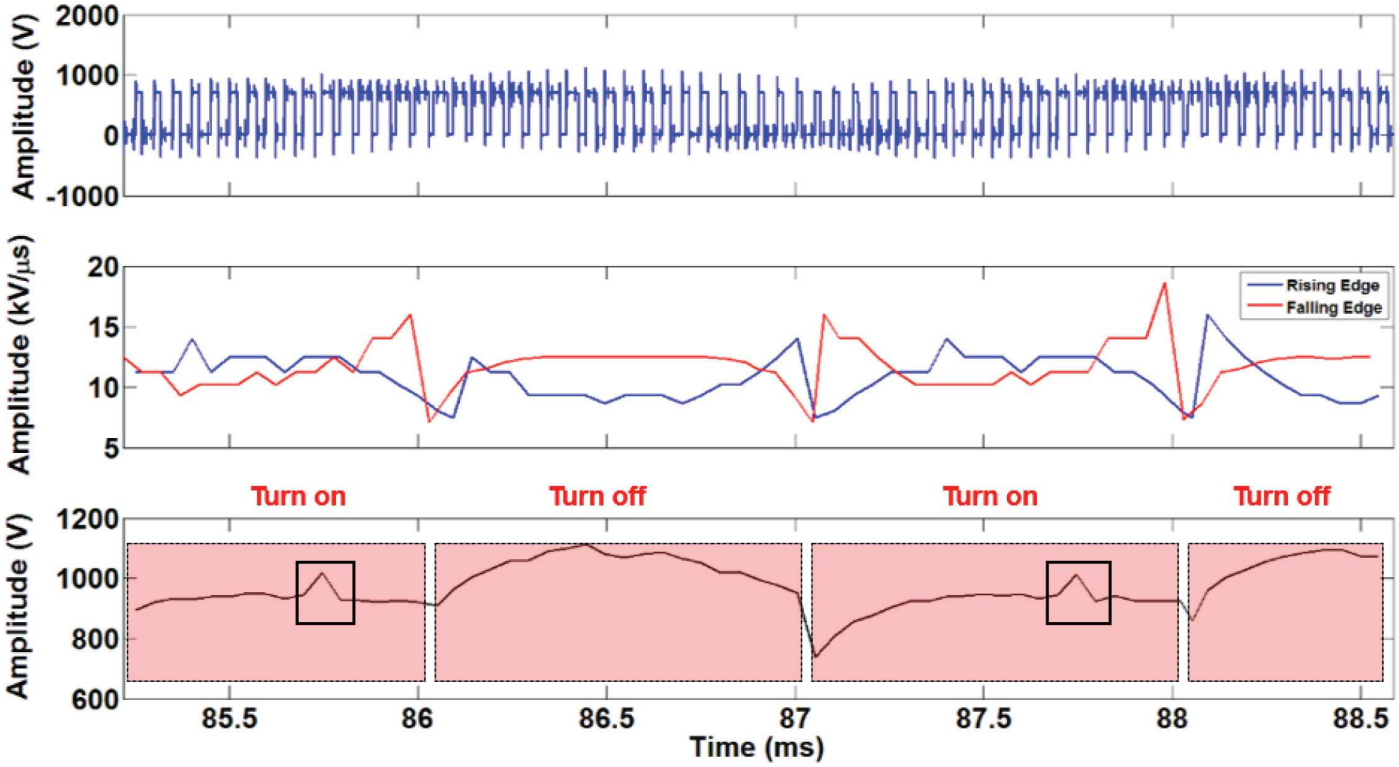


Figure 3. Rise time and falling time of edge for turn-on only and overvoltage measurement

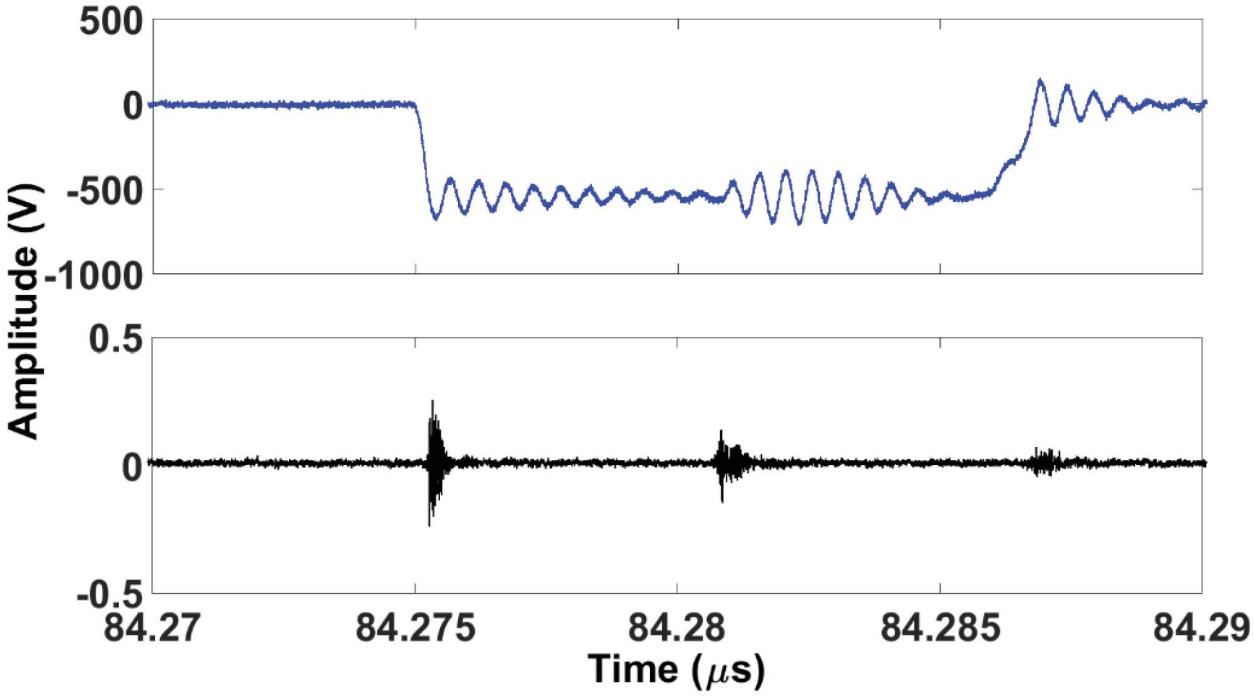


Figure 4. Zoom on turn-on and turn-off phase to phase voltage with sensor signal (below)

## Non-Intrusive Sensor Performance in Motor Supplied by SiC PWM Inverter

### *Capacitive Sensor Study*

Thanks to the capacitive effect, partial discharge small current impulses are transduced into voltage variations through the capacitance between the copper wire and oscilloscope impedance.

The Jack-SMA sensor is a robust, inexpensive, and standardized way of detection PD in a non-intrusive way. But, for consistency to be achieved, the positioning of the sensor has to be ensured. Due to its small geometry, achieving good contact and adequate holding on the power cable can be complex. For this reason, we developed special 3D printed pliers to ensure good contact regardless of the cable gauge and vibrations

The sensor is based on a capacitive coupling. Sensor sensitivity can therefore be increased simply by improving the coupling capacitance value. This is achieved by increasing the contact surface by putting copper tape on the surface of the power cable to control the interacting area and thus the value of the induced capacity (Fig 7).

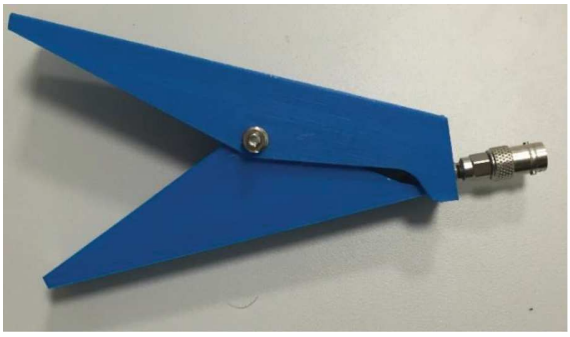

Figure 5. Jack-SMA with the holding system

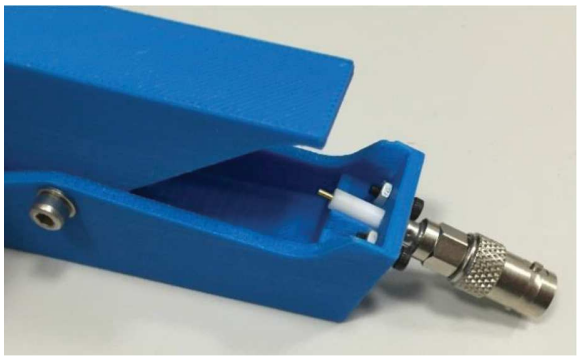

Figure 6. Zoom on the connection part

It is important to note that this sensor is sensitive to the dynamic of the partial discharge compared to the "standards" sensors, which are only sensitive to the amplitude of the discharge.

### *Switching Noise Magnitude Evolution: Relation with Common Mode Current*

When performing non-intrusive PD detection, periodic pulses interference of high frequency content are often the major source of noise and need to be filtered. Before using any filtering, analog or numeric, it is important to track how maximum switching noise is evolving with DC bus voltage. It is expected that a higher DC bus will lead to a higher switching noise during the rise and will thus hide potential partial discharge signals.

From Fig.4, a typical sequence of switching could be observed with; from left to right, a turn off, a parasitic response from a switching on another phase and a slow turn-on. Each of these switching is associated with a different switching noise detected by our non-intrusive sensor.

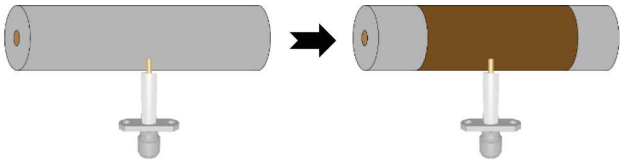

Figure 7. Optimization of the sensor sensitivity

This source of noise collected by the sensor is dependent of the common mode capacitance of the whole set-up value. Indeed, since the non-intrusive sensor relies on capacitive effect to collect the partial discharge towards the input impedance of the oscilloscope and its low voltage potential; it should also collect a part of the common mode current created by switching.

The whole set-up common mode capacitance is greatly increased when the stator frame is connected to ground, thus offering a low impedance path for high frequencies common mode current. Whereas the common mode capacitance is decreased when stator frame is floating. In other words, the common mode current seen by the sensor will be low when the stator frame is grounded, as it is usually the case in aeronautic applications.

The sensitivity of the measurement of PD pulse high frequency current will thus be function of the sample common mode capacitance, detection capacitance and the spread of frequency content between switching common mode current and partial discharge current.

The following measurements (Table 2) were made while feeding a three phases stator with the inverter drive with the sensor without an increase of the capacitive effect to evaluate the amplitude of common mode noise and highlight this effect.

When an the detection capacitance is increased, the common mode current for switching is greatly increased when the stator is floating and increased voltage limit of oscilloscope input of 5V under 50Ω impedance. (Table 3)

Table 2. Measurement sensitivity

| DC Bus | Vmax (peak to peak)<br>Grounded stator | Vmax (peak to peak)<br>Floating stator |
|---|---|---|
| 50V | 26 mV | 33 mV |
| 100V | 52 mV | 66 mV |
| 200V | 103 mV | 151 mV |
| 300V | 137mV | 186 mV |
| 400V | 169mV | 206mV |
| 500V | 197 mV | 230 mV |
| 540V | 208 mV | 234 mV |
| 600V | 233 mV | 248 mV |
| 700V | 276 mV | 286 mV |

Table 3. Measurement sensitivity with increased capacitance

| DC Bus | Vmax (peak to peak)<br>Floating stator + increased capacitance | Vmax (peak to peak)<br>Floating stator |
|---|---|---|
| 50V | 1.01V | 33 mvV |
| 100V | 2.07V | 66 mV |
| 200V | 3.87V | 151 mV |
| 300V | 4.81V | 186 mV |
| 400V | Overload (max 5V) | 206mV |

### *Analogical Filters Performance*

Since the sensor is sensitive to quick changes in current, any phenomenon that induces this type of variation can cause a sensor response. When seeking to detect PDs in equipment supplied by inverter using PWM., a key challenge is to distinguish the raw signal with respect to electromagnetic noise induced by fast switching inverters. The magnitude of the signal associated with partial discharges generally has an amplitude of several tens of mV, while the magnitude of the noise signal is on the order of several hundred mV and depends on the voltage magnitude as has been demonstrated previously.

From a frequency perspective, the spectrum of a discharge may extend up to the GHz range, while the noise spectrum does not extend beyond a few hundred of MHz. The filter cutoff frequency should be greater than the frequency for noise suppression of commutations and must be adapted to the voltage rise time.

In our work, a simple technique for observing the presence or the absence of a discharge was to filter the raw signal in order to retrieve only the high-frequency components of the signal using analog high-pass filters. While this technique works well, some external parameters can alter the discharge spectrum like the pressure.

It is therefore important to determine the amplitude of the noise induced by the switching, detected by the sensor. A study was carried out for different values of DC bus and for different cut-off frequency of high-pass filters. These tests were carried out at a switching frequency of 20 kHz and a carrier frequency of 1 kHz using the increased capacitance.

It can be seen in Fig. 8 that the noise increases with the amplitude of the DC bus, as previously, but does not change linearly once filtered. This is explained by the fact that the dV / dt is not only dependent on the amplitude of the voltage but also the switched current. It can be seen that for a cutoff frequency greater than 100 MHz much of the noise seems to be suppressed since the noise does not exceed 10 mV. Beyond 200 MHz all noise is suppressed, the remaining noise is white noise induced by the oscilloscope. It is thus recommended, for this inverter drive, this harness and this sample, to use a 200MHz analog filter with the increased capacitance.

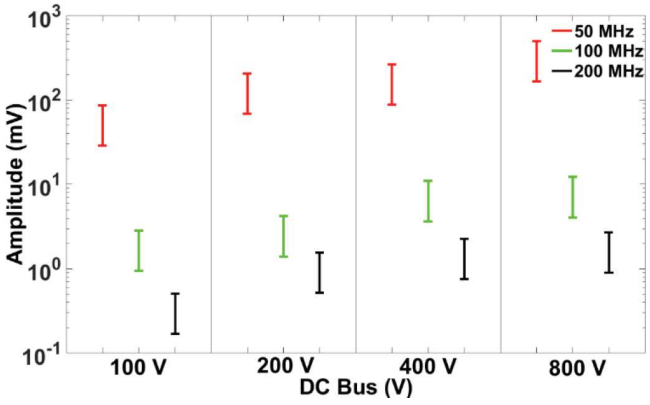


Figure 8. Influence of DC bus voltage and filter cut-off frequency on noise amplitude

### *Noise Suppression Improvement*

In aeronautical environments, some equipment operates under pressure and temperature conditions that can vary greatly. These environmental condition variations can alter the signals associated with PD. The denoising technique must therefore work regardless of the operating conditions. The choice of the cutoff frequency remains a difficult task because it is dependent on the analog filters available during testing, of the pressure as observed above as well as the expertise of the operator. It thus seems important to optimize filter choice. To do this, it is possible to use digital filters that make it possible to have an infinite number of filters available. However, this solution still requires significant expertise regarding the selection of the filter cutoff frequency. This is why it is necessary to develop a fully automated digital method to replace the expertise of an operator. We therefore decided to use the wavelet transform method.

Invented by Jean Morlet, the wavelet transform (Wavelet Transform - WT), just as the Fourier transform (Fourier Transform - FT) is a mathematical signal processing tool that decomposes a signal into different basic functions. The basic functions of the FT being the sine and cosine, the result of applying this method provides information only on the frequency content of the signal of interest. The disadvantage lies in not knowing the moment at which each frequency component appears. Besides that, the basic functions of the WTs called “wavelets” allow two-dimensional resolution in the frequency and time domains. The result of these two transforms represents the projection of a signal based on wavelets for the WT or complex exponential functions for the FT. Moreover, in comparison, the FT shows extreme efficiency for analyzing periodic phenomena, time-invariant and stationary techniques, while WT screens all components produced by transients, of variable time and non-stationary [15], [17].

Therefore, with the PD signal being of a non-periodic nature and exhibiting very fast transient characteristics, the WT approach seems more suitable in this context. The method has proved its ability to denoise PD signals, but mainly under AC voltage and in the presence of white noise [16], [18], [19], [20]. It is therefore necessary to check whether this method is functional for denoising PDs occurring under PWM. We used this technique to remove noise superimposed on PDs.

We therefore compared the results given through an analog high-pass filtering, and those given by the wavelet transform. For this the ignition of PDs was observed on a stator supplied by a SiC inverter with a 20 kHz switching frequency and a 1 kHz carrier frequency. The stator (n°2) was positioned in a vacuum chamber in order to carry out tests at atmospheric pressure and at low pressure.

First, we observed the noise associated with switching at atmospheric pressure.

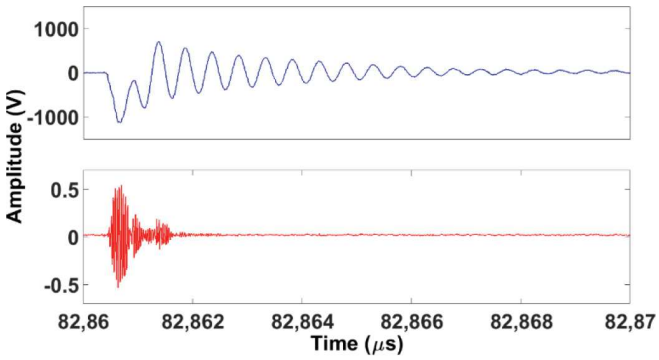


Figure 9. PWM voltage (blue), sensor signal without filtering (red)

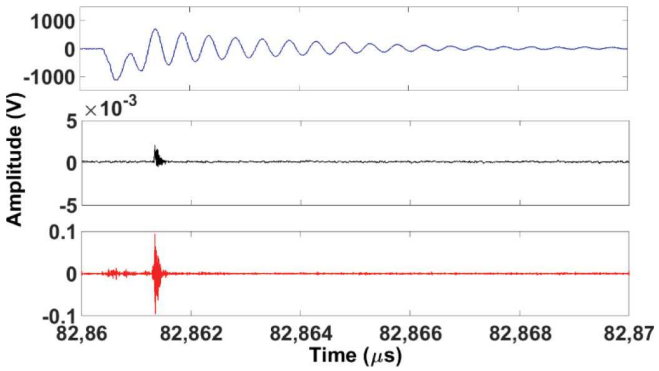


Figure 10. PWM voltage (blue), sensor signal filtered at 200 MHz (black), PD signal reconstructed by CWT (red) at atmospheric pressure

It can be observed in Fig.9 that the noise amplitude is greater than 500 mV and corresponds temporally to the switching. In this case, there are two close switching. The oscillations associated with the first switching are not stabilized when the second switching occurs, this results in a potential difference much greater than the DC bus which can lead to the appearance of PDs.

It can be seen in Fig.10 that the noise associated with the first switching is completely suppressed for the two filtering techniques. A signal can then be seen which corresponds temporally to the greatest potential difference. These signals correspond to a PD, and it can be seen that the signal reconstructed by the wavelet transform has an amplitude twenty times greater than the signal filtered analogically. The method is functional and allows to recover a signal with a much higher Signal to Noise Ratio (SNR).

It is now important to check the method at low pressure (100 mbar).

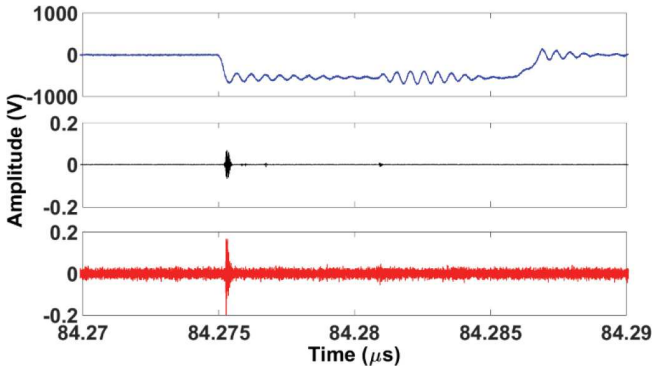


Figure 11. PWM voltage (blue), sensor signal filtered at 200 MHz (black), PD signal reconstructed by CWT (red) at 100 mbar

One can see in Fig.11 that the method is able to detect PDs 100 mbar, however in this case the amplitude of the signal is only two times greater than the filtered analogical signal.

The digital denoising method based on continuous wavelet transform is functional. Moreover this method sets all the wavelet transform configuration parameters automatically [21]. This method has real interest with respect to high-pass filtering because human expertise is no longer required to remove noise in signals. It is still important to note the limitations of this technique. First, to be functional, it is necessary for the signal to be discretized with a large sampling frequency in order to represent fast signals.

Another important point is that the amplitude of the signal reconstructed by the method has a very significant error. Indeed, frequency band overlap corresponding to each level of decomposition also induces a very significant error on the pulse wave shape. However, error is also induced with the use of a high-pass filter because all frequency components below the cutoff frequency are removed or attenuated. It has also been reported that PD pulse shape is distorted by such analog filtering.

As a conclusion, the use of both analog filtering and numerical processing based on wavelet transform allows the detection of PDIV under SiC pulse at both atmospheric and reduced pressure.

It should be noted that although PDIV could be determined with this method, no calibration or PD pulse shape analysis could be carried out at the moment with the proposed algorithm. Indeed, due to the dependency of the sensor to the derivative of the current pulse rather than being a simple proportional impedance, the charge of the discharge current would have to be doubly integrated which is further complicated by the fact the parasitic oscillations of the circuit in response to the PD pulse.

## Electric Motors Description

In order to validate our detection method and to make the best use of our test bench based on the SiC technology, three low voltage stators (max 540V DC) with insulation different characteristics have been chosen of designed. The table below summarizes some of their properties.

These are stators of three-phases Permanent Magnet Synchronous Motor (PMSM), they are designed to be powered with Pulse Width Modulation (PWM) inverters. (Table 4)

Table 4. Stators main characteristics

| | Stator n°1 | Stator n°2 | Stator n°3 |
|---|---|---|---|
| Power | 10kW | 15kW | 60kW |
| DC Voltage | 540Vdc | 540Vdc | 400Vdc |
| Impregnation | No | Yes | Yes |
| End-winding compression | No | Yes | No |
| Manufacturing | Manual | Manual | Automatic |

### *Stator n°1: Laboratory Dummy Sample*

The design of this stator has been extensively detailed in [6] are tables regarding insulation and electric design are recalled below (Tables 5, 6, 7). The two terminals of each of his three phases are accessible. This allows to test each phase separately. It is very important to highlight that the stator is not impregnated and that it has been rewound before starting the test campaign to ensure a PD free previous history. (Fig. 12)

Figure 12. Stator 1: IRT Saint Exupéry typical HVDC stator

Table 5. Stator n°1 winding characteristics

| | |
|---|---|
| Number of phases | 3 |
| Number of slots | 24 |
| Number of poles | 8 |
| Coil pitch | 1 - 4 |
| Ø copper wire [mm] | 0,5 |
| Number of strands in // | 2 |
| Number of turns per coil | 78 |
| number of wires per slot | 156 |
| Number of way in // | 4 |
| Number of coil per slot | 1 |
| Coupling | Star |

Table 6. Enamel wire properties (Norm IEC 60317-13)

| | | |
|---|---|---|
| Copper diameter [mm] | | 0,5 ±0,005 |
| Grade | | 2 |
| Class | | H |
| Magnet wire diameter [mm] | Minimum | 0,545 |
| | Maximum | 0,566 |
| Voltage breakdown [V] | | 4600 |

Table 7. Insulation system reference and thickness for stator n°1

| Insulation type | | Reference | Thickness [mm] |
|---|---|---|---|
| Phase to ground | Slot cell | NOMEX 410- Class H | 0,15 |
| | Wedge | ISOVALFR4-Class H | 0,5 |
| Phase-to-phase | | INTERTAPE-Class H | 0,065 |
| Coils connections and phase terminal | | Siligaine – Class H | 0,2 |

### *Stator n°2: High Mechanical Integration Constraint Stator*

Compared to the first stator, this one is impregnated under vacuum pressure (VPI process), this allows the varnish to penetrate as much as possible within the windings. Its end-windings are mechanically compressed to optimize the axial length of the machine (Fig. 13). The neutral point is not accessible so the evaluation of the PDIV of each phase alone (turn to turn PDIV) is not possible. Therefore, only the star-connected case will be tested.

Due to non-disclosure agreement with our industrial partners, insulation and electrical design details could not be provided for stator n°2 except that this is a three phases motor with four parallel coils per phase. The winding diagram of stator n°2 is similar to stator n°1.

Figure 13. Stator n°2 - Compact stator

### *Stator n°3: Low Cost Stator*

Unlike the other two stators, this stator is cooled by air. The insertion of its coil is automated, this allows a more reproducible winding but with a slightly lower filling factor compared to the other stators. The end-windings are not compressed and are insulated by relatively thick tapes. It is also varnished using dipped impregnation instead of vacuum pressure impregnation as shown in Fig. 14

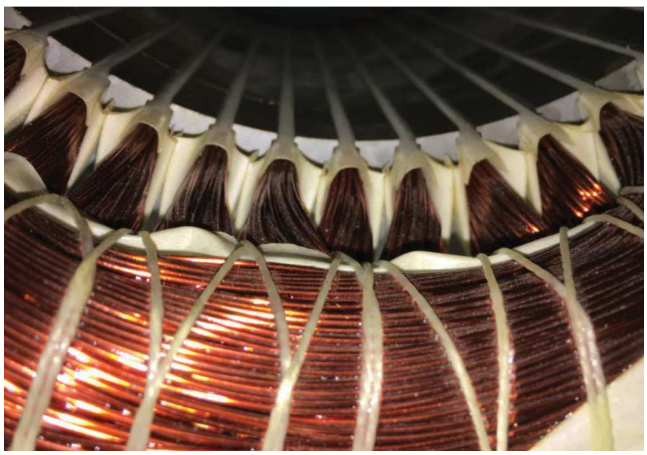

Figure 14. Details of stator n°3- Traction motor

Each of its three phases (U, V and W) is composed of four coils (U1, U2, U3, U4, V1, V2, V3, V4 and W1, W2, W3, W4). These are accessible and can be connected in different ways easily although the nominal star connected configuration is with four coils in parallel for each phases. This stator is designed for electric traction application under atmospheric conditions. Therefore, the proposed tests don't consider the effect of pressure.

## Advanced Partial Discharge Testing Results

### *General Purpose*

For each stator studied, AC and SiC PWM tests were carried out at both 100mbars and atmospheric pressure except for stator n°3. The purpose of these tests is to investigate the PDIV under SiC inverter drive electrical stress compared to typical AC tests usually carried out. On one hand, AC tests are used to determine the PDIV between phases (if neutral point is disconnected), and between phases and stator frame. On the other hand, SiC inverter tests will be used to determine PDIV in a more realistic approach with fast rime time impulse compared to aeronautic standard (>5V/µs).

### *PDIV of Experimental Set-Up*

Before starting any investigation, PDIV of the experimental set-up without any sample is determined under 50 Hz AC voltage. (Table 8)

Table 8. Experimental set-up PDIV

| Experimental set-up PDIV | |
|---|---|
| Atmopsheric pressure | 3000 Vpeak |
| 100 mbars | 1500 Vpeak |

### *Stator n°1*

Stator n°1 has been designed at IRT Saint-Exupery to represent a typical aeronautic electric motor insulation system.

## Phase to ground

In the first test, all phases are star-connected and the stator frame is grounded to test the slot insulation only. Then each phase is tested separately in respect to the stator frame. Tests are performed with 50 Hz AC voltage (Table 9)

Table 9. Phase to ground AC Partial Discharge tests for stator n°1

| **All phases connected and stator grounded** | | |
|---|---|---|
| Pressure | Atmospheric pressure | 100 mbars |
| PDIV (peak) | 1450V peak | 675 V peak |
| PDIV (RMS AC) | 1026V RMS | 477V RMS |
| Standard dev. | 39V RMS | 22V RMS |
| % Standard dev/mean | 3.8% | 4.7% |
| Number of tests | 17 | 17 |
| 95% confidence bounds | [948-1104] V RMS | [432-522] V RMS |
| **Phase U and stator frame floating** | | |
| Pressure | Atmospheric pressure | 100 mbars |
| PDIV (peak) | 1466V peak | 685 V peak |
| PDIV (RMS AC) | 1036V RMS | 484V RMS |
| Standard dev. | 31V RMS | 9V RMS |
| % Standard dev/mean | 3% | 1.8% |
| Number of tests | 17 | 17 |
| 95% confidence bounds | [973-1100] V RMS | [466-502] V RMS |
| **Phase V and stator frame floating** | | |
| Pressure | Atmospheric pressure | 100 mbars |
| PDIV (peak) | 1462V peak | 662 V peak |
| PDIV (RMS AC) | 1033V RMS | 468V RMS |
| Standard dev. | 31V RMS | 29V RMS |
| % Standard dev/mean | 3% | 6% |
| Number of tests | 17 | 17 |
| 95% confidence bounds | [971-1095] V RMS | [410-526] V RMS |
| **Phase W and stator frame floating** | | |
| Pressure | Atmospheric pressure | 100 mbars |
| PDIV (peak) | 1474V peak | 670 V peak |
| PDIV (RMS AC) | 1042V RMS | 474V RMS |
| Standard dev. | 34V RMS | 16V RMS |
| % Standard dev/mean | 3.3% | 3.4% |
| Number of tests | 17 | 17 |
| 95% confidence bounds | [973-1110] V RMS | [442-506] V RMS |

Results are similar with our previous technical report [6], showing that even a complete rewound of the electric motor lead to stable PDIV performance regarding the slot insulation. Few variations between phases could be noted suggesting that slot insulation is balanced in all slots.

## Phase to Phase

The phase to phase insulation is now tested, with two phases grounded and one with AC 50 Hz voltage while the stator frame is floating. (Table 10)

Again, results are similar with our previous technical report [6], with very few variations between what seems to be a balanced phase to phase electrical insulation. On average, the phase to phase insulation is also weaker than the phase to ground insulation system.

Table 10. Phase to phase AC Partial Discharge tests for stator n°1

| **Phase U / Phase VW and stator frame floating** | | |
|---|---|---|
| Pressure | Atmospheric pressure | 100 mbars |
| PDIV (peak) | 1160V peak | 642 V peak |
| PDIV (RMS AC) | 819V RMS | 454V RMS |
| Standard dev. | 23V RMS | 12V RMS |
| % Standard dev/mean | 2.8% | 2.8% |
| Number of tests | 17 | 17 |
| 95% confidence bounds | [773-866] V RMS | [429-480] V RMS |
| **Phase V / Phase UW and stator frame floating** | | |
| Pressure | Atmospheric pressure | 100 mbars |
| PDIV (peak) | 1110V peak | 628 V peak |
| PDIV (RMS AC) | 784V RMS | 444V RMS |
| Standard dev. | 38V RMS | 10V RMS |
| % Standard dev/mean | 4.8% | 2.2% |
| Number of tests | 17 | 17 |
| 95% confidence bounds | [708-861] V RMS | [424-464] V RMS |
| **Phase W / Phase UV and stator frame floating** | | |
| Pressure | Atmospheric pressure | 100 mbars |
| PDIV (peak) | 1100V peak | 630 V peak |
| PDIV (RMS AC) | 778V RMS | 445V RMS |
| Standard dev. | 24V RMS | 15V RMS |
| % Standard dev/mean | 3.1% | 3.5% |
| Number of tests | 17 | 17 |
| 95% confidence bounds | [730-826] V RMS | [414-480] V RMS |

## SiC Inverter Drive Test

Unfortunately, an insulation failure during preliminary tests prevents us from reporting the complete set of results under impulse test. The failure occurred at 100 mbars of pressure, stator frame floating under a 700V DC bus with all phases star connected.

Initially, PDIV with these conditions was around 460-500V DC (650-700 Vpeak) bus at 100 mbars. Voltage was increased above PDIV to observe partial discharge evolution electrically and optically to rule out possible false positive signals. The weak point was identified to be the exit of the slot and within end-winding. The failure occurred quite quickly (about half-an-hour of equivalent testing time above PDIV) at th identified weak point and a picture of the failure is reported. (Fig. 15)

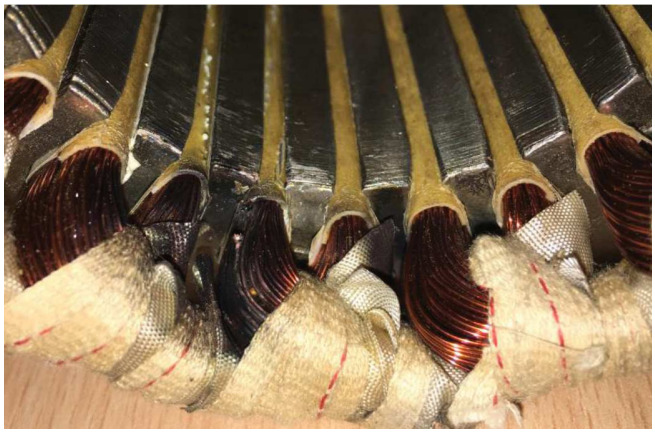

Figure 15. Stator n°1 failure at 100 mbars

PDs eventually led to an electrical arc between phases (short circuit) causing magnet wire to melt, and finally to be completely cut. It is believed that the electrical arc even hang to the stator frame

(floating). It should be noted that stator frame are usually not floating in aeronautic electromechanical chain which could have cause another failure mechanism or more damage.

## *Stator n°2*

Stator n°2 is also an aeronautic electric motor with the neutral point star connected meaning only few tests are possible both in AC and with the SiC inverter drive. For example, phase to phase tests are not possible.

### Phase to Ground Tests

A typical phase to ground insulation test is made on all phases at the same time with the stator frame grounded at 50Hz AC voltage

Phase to ground insulation performance is better than for stator n°1 which presents similar insulation characteristics except for test for the VPI varnishing process. It is believed that the VPI process helps increase the PDIV between slot and phases by ensuring varnish fill most of air gaps.

### Stator Supplied by Three-Phase SiC Inverter at Atmospheric Pressure

The electric stator is fed with the inverter drive at atmospheric pressure with a short harness with a typical operating point.

Table 11. Phase to ground AC Partial Discharge tests for stator n°2

| All phases and stator grounded | | |
|---|---|---|
| Pressure | Atmospheric pressure | 100 mbars |
| PDIV (peak) | 1626V peak | 676 V peak |
| PDIV (RMS AC) | 1150V RMS | 478V RMS |
| Standard dev. | 29V RMS | 16V RMS |
| % Standard dev/mean | 2.5% | 3.5% |
| Number of tests | 17 | 17 |
| 95% confidence bounds | [1091-1208] V RMS | [444-511] V RMS |

Table 12. SiC inverter drive operating point

| | |
|---|---|
| Switching frequency | 20 kHz |
| Carrier frequency | 2000 Hz |
| Modulation factor | 0.3 |
| Harness length | 1 m |

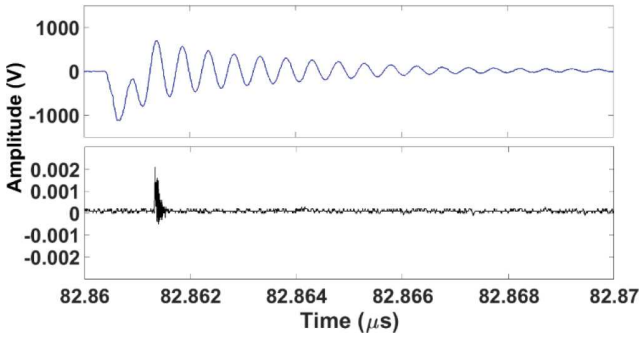


Figure 16. PWM voltage (blue), sensor signal filtered at 200 MHz (black) at atmospheric pressure

The non-intrusive sensor is positioned on one of the power cable (harness) feeding the electric stator with an increased capacitive effect as explained earlier in this article. A 200MHz high-pass filter is used to perform PD detection. Although not reported in details here, a higher cut-off frequency could be used with similar results.

Fig. 16 is a typical case with a PD signal appearing for the maximum peak to peak voltage (1410V peak-peak) for a short impulse case. It should be noted that this PD location suggests a turn-to turn or a phase to phase default. Indeed, a phase to ground PD is highly unlikely because the peak voltage does not increase above 1000V, which is lower than phase to ground PDIV under AC voltage reported in Table 11. On the contrary, a turn default could be tested with SiC impulse around 10kV/µs.

### Stator Supplied by Three-Phase SiC Inverter at Atmospheric Pressure

The electric stator is tested at low pressure (100mbars). PDIV is also evaluated with a high-pass filter of 200MHz in the same manner.

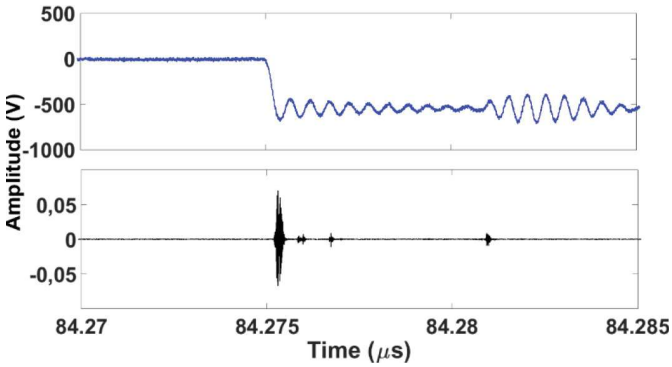


Figure 17. PWM voltage (blue), sensor signal filtered at 200 MHz (black) at 100 mbar

Table 13. Phase to ground AC Partial Discharge tests for stator n°2

| Three phases | |
|---|---|
| Atmopsheric pressure | 1410 Vpeak-peak [1325-1494V] peak 95% confidence bounds |
| 100 mbars | 640 Vpeak [600-680V] peak 95% confidence bounds |

It can be seen on Fig. 17 that the discharge appears at 641 Vpeak at 100 mbar for the maximum voltage. Any insulation could trigger a This PD location is not characteristics of any insulation on the contrary to the previous case. Other parasitic signals of lower amplitude at 100 mbar could be observed and are labelled as residual noise. As a summary (Table 13), these tests prove that non-intrusive PD detection is possible at both atmospheric and low pressure on electric stator fed by a SiC inverter drive. Detection with high-pass filtering was confirmed with visual observation of the stator during test and numerical signal processing.

## *Stator n°3*

Stator n°3 is only tested at atmospheric pressure

### Phase to Ground

Phase to ground tests are performed at 50 Hz AC voltage

Table 14. Phase to ground AC Partial Discharge tests for stator n°3

| **All phases connected and stator grounded** | |
|---|---|
| PDIV (peak) | 1460V peak |
| PDIV (RMS AC) | 1032V RMS |
| Standard dev. | 37V RMS |
| % Standard dev/mean | 3.6% |
| Number of tests | 17 |
| 95% confidence bounds | [957-1107] V RMS |
| **Phase U and stator frame floating** | |
| Pressure | Atmospheric pressure |
| PDIV (peak) | 1466V peak |
| PDIV (RMS AC) | 1037V RMS |
| Standard dev. | 22V RMS |
| % Standard dev/mean | 2.1% |
| Number of tests | 17 |
| 95% confidence bounds | [991-1082] V RMS |
| **Phase V and stator frame floating** | |
| Pressure | Atmospheric pressure |
| PDIV (peak) | 1570V peak |
| PDIV (RMS AC) | 1110V RMS |
| Standard dev. | 33V RMS |
| % Standard dev/mean | 3% |
| Number of tests | 17 |
| 95% confidence bounds | [1042-1178] V RMS |
| **Phase W and stator frame floating** | |
| Pressure | Atmospheric pressure |
| PDIV (peak) | 1528V peak |
| PDIV (RMS AC) | 1080V RMS |
| Standard dev. | 15V RMS |
| % Standard dev/mean | 1.4% |
| Number of tests | 17 |
| 95% confidence bounds | [1050-1111] V RMS |

In table 14, PDIV values for each phase are more widely distributed regarding stator n°3 than for both previous stators which is interesting given its automated winding process. A lower filling ratio for stator n°3 may be another cause for such difference regarding phase-to-ground insulation performance. Lowest phase to ground PDIV for stator n°3 is very similar to stator n°1 average phase to ground PDIV value.

### Phase to Phase

The phase to phase insulation is made with the same material as the slot insulation (insulating paper). Results (Table 15) are consistent with this observation and should lead to better phase-to-phase insulation performance, although PDIV value are also more widely distributed. Another possible cause for this better performance is the winding configuration with clearly segregated electric poles typical of concentric windings.

Table 15. Phase to phase AC Partial Discharge tests for stator n°3

| **Phase U / Phase VW and stator frame floating** | |
|---|---|
| Pressure | Atmospheric pressure |
| PDIV (peak) | 1480V peak |
| PDIV (RMS AC) | 1046V RMS |
| Standard dev. | 15V RMS |
| % Standard dev/mean | 1.5% |
| Number of tests | 17 |
| 95% confidence bounds | [1014-1078] V RMS |
| **Phase V / Phase UW and stator frame floating** | |
| Pressure | Atmospheric pressure |
| PDIV (peak) | 1531V peak |
| PDIV (RMS AC) | 1083V RMS |
| Standard dev. | 37V RMS |
| % Standard dev/mean | 3.5% |
| Number of tests | 17 |
| 95% confidence bounds | [1007-1158] V RMS |
| **Phase W / Phase UV and stator frame floating** | |
| Pressure | Atmospheric pressure |
| PDIV (peak) | 1603V peak |
| PDIV (RMS AC) | 1133V RMS |
| Standard dev. | 29V RMS |
| % Standard dev/mean | 2.5% |
| Number of tests | 17 |
| 95% confidence bounds | [1075-1191] V RMS |

### Coil-to-Coil Tests

Since 12 coils are available, each one is tested relatively to each other within each phase. This is not a conventional test since these coils are supposed to be connected in parallel within each phase and should not see great voltage difference relatively to each other. Two case could appear in the winding depending on the configuration. Either coils of the same phase are in close vicinity to each other and the magnet wire and varnish is the only insulation and it could lead to a fairly low PDIV if the start of one coil is close to the end of the other. Or coils are wide away meaning that PDIV should be very high compared to other insulation.

For the sake of brevity not all statistical indicators are reported here but a standard deviation of 3% is representative of the accuracy of PDIV evaluation in table 16.

On the whole, three very different situations have been observed.

Phase U presents the lowest coil to coil insulation of all phase at atmospheric pressure with a lot of variation between configurations. This weakness obviously does not appears with AC test because all coils are at the same voltage. This may be explain by the fact that this motor has already be tested numerous time regarding partial discharge level with an inverter.

On the contrary, phase V presents the higher PDIV between coils (above 2kV peak) whereas phase W only shows one weakness between W1 and W4 which will be very useful later on.

Table 16. Phase to phase AC Partial Discharge tests for stator n°3

| **Phase U** (white) | |
|---|---|
| Coil configuration | PDIV |
| U1/U2 | 1125 Vpeak |
| U1/U3 | 1000 Vpeak |
| U1/U4 | 1700 Vpeak |
| U2/U3 | 1860 Vpeak |
| U2/U4 | 1060 Vpeak |
| U3/U4 | 1090 Vpeak |
| **Phase V (blue)** | |
| Coil configuration | PDIV |
| V1/V2 | >2000 Vpeak |
| V1/V3 | >2000 Vpeak |
| V1/V4 | >2000 Vpeak |
| V2/V3 | >2000 Vpeak |
| V2/V4 | >2000 Vpeak |
| V3/V4 | >2000 Vpeak |
| **Phase W (black)** | |
| Coil configuration | PDIV |
| W1/W2 | >2000 Vpeak |
| W1/W3 | >2000 Vpeak |
| W1/W4 | 1260 Vpeak |
| W2/W3 | >2000 Vpeak |
| W2/W4 | >2000 Vpeak |
| W3/W4 | >2000 Vpeak |

## Coil Configurations and Electric Stator Characteristics

In order to evaluate all potential configurations offered to designers to meet required insulation and electrical specifications, we will try to take advantage of having access to its 12 coils and connect them to each other's. Three configurations are provided below: for studies

- 4 coils in series : Configuration 1(Fig.17)
- (2 coils in series) // (2 coils in series) : Configuration 2 (Fig.18)
- And 4 coils in parallel : Configuration 3 (Fig.18)

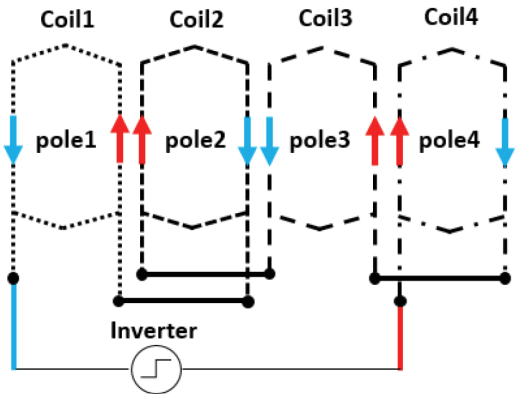


Figure 18. Configuration 1: 4 coils in series

The number of turns in series per phase of configuration 3 is equal to twice that of configuration 2 and equal to four times that of configuration 1.

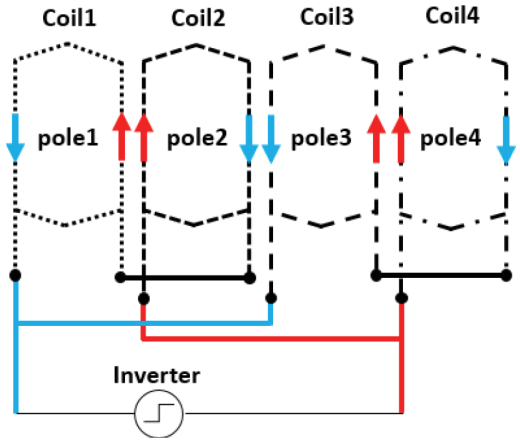


Figure 19. Configuration 2: (2 coils in series) // (2 coils in series)

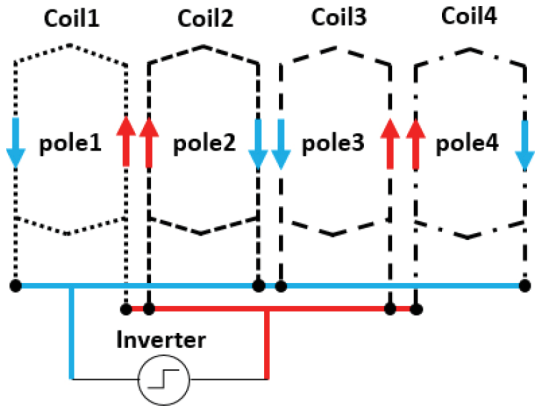


Figure 20. Configuration 3 : 4 coils in parallel

In terms of functional performance, the number of turns per phase plays a major role in the design process of an electrical machine. It impacts linearly the level of Back EMF (Fig. 20), therefore the base speed ($\Omega_b$) of the machine. $\Omega_b$ represents the speed from which the constant power operating mode begins (flux Weakening mode in the case of PMSM). It also impacts the torque coefficient and consequently the current consumed by the motor.

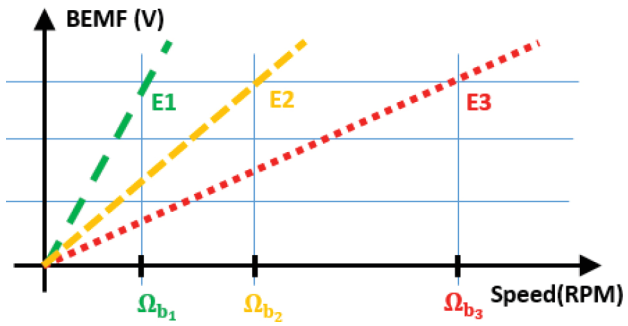


Figure 21. Back EMF in function of winding configurations: E1 for configuration1, E2 for configuration2 and E3 for configuration3

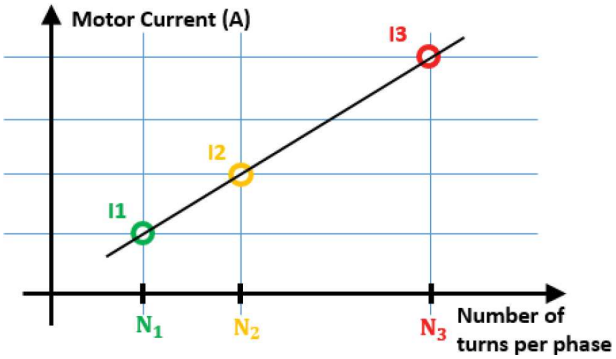


Figure 22. Motor nominal current in function of winding configurations: I1 for configuration1, I2 for configuration2 and I3 for configuration3

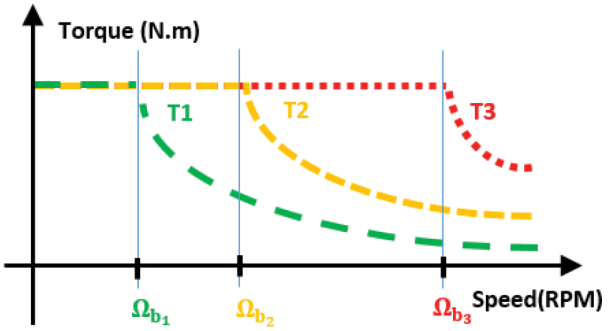


Figure 23. Electromagnetic torque in function of winding configurations: T1 for configuration1, T2 for configuration2 and T3 for configuration3 (Analysis valid for the same DC voltage)

Compared to the nominal current of the first configuration, the nominal current of the second one is twice smaller and that of the third one is four times smaller (Fig.21). The maximum torque is often the most dimensioning parameter. In the three proposed winding configurations, the motor will provide the same maximum torque with slightly the same energetic efficiency (Fig.22).

## SiC Inverter Drive Tests

In this case, the four coils of each phase were connected in parallel (configuration 3) and each phase is tested separately between its start and the neutral point with a SiC PWM waveform (see table 17 for operating point). For the nominal case, the neutral point is start connected and the stator frame at a floating potential and the SiC inverter drive is feeding the three phases at the same time with a PWM waveform.

From the result table 18, it seems that each phase has the same PDIV under SiC impulse stress, namely around 1300V peak. In the nominal case when all phases are star-connected, the PDIV could not be determined which is consistent with the fact that the most stressing case is when only one phase is tested. Indeed, when all phases are star-connected, each phases is facing a 2/3 of the voltage at maximum under a PWM waveform.

When comparing results with coils results for phases V and W one could observe that it is likely that phase V presents a turn-to turn PD whereas phase W presents a coil-to coil PD. Impulse tests have to be performed coil by coil for phase V and W to define accurately PD location.

Table 17. Phase to ground AC Partial Discharge tests for stator n°3

| | |
|---|---|
| Switching frequency | 20 kHz |
| Carrier frequency | 2000 Hz |
| Modulation factor | 0.3 |

Table 18. Phase to ground AC Partial Discharge tests for stator n°3

| SiC inverter drive phase tests | |
|---|---|
| Phase U – Neutral point | 1320 Vpeak [1240-1400] Vpeak with 95% confidence bounds<br><br>DC Bus : 820V<br>Overshot : 500V<br>Rise time : 220ns<br>dV/dt : 6kV/µs |
| Phase V – Neutral point | 1300 Vpeak [1220-1380] Vpeak with 95% confidence bounds<br><br>DC Bus : 800V<br>Overshot : 500V<br>Rise time : 220ns<br>dV/dt : 5.9kV/µs |
| Phase W – Neutral point | 1280 Vpeak [1200-1350] Vpeak with 95% confidence bounds<br><br>DC Bus : 770V<br>Overshot : 490V<br>Rise time : 220ns<br>dV/dt : 5.8kV/µs |
| Nominal case | >1000V DC bus (>1600Vpeak) |

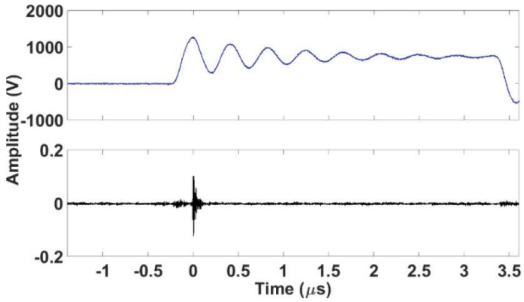


Figure 24. PWM voltage (blue), sensor signal filtered at 200 MHz (black) at atmospheric pressure on stator n°3

Table 19. Phase to ground AC Partial Discharge tests for stator n°3

| **Impulse test on each coil of phase W (black)** | |
|---|---|
| Coil | PDIV |
| W1 | >1600 Vpeak |
| W2 | >1600 Vpeak |
| W3 | >1600 Vpeak |
| W4 | >1600 Vpeak |

The results in table 19 confirm that coil-to-coil insulation was actually tested when applying SiC impulse on phase W. In fact, the phase test presents a slightly higher PIDV than the W1/W4 coil

PDIV. This is an interesting result because it shows that depending on the winding configuration and coils arrangement (4 in parallel), PDs could also appear between coils of the same phase.

Results (Table 20) from SiC impulse tests on phase V confirm the assumption that phase V is presenting turn-to-turn PD on coil V2. It should be noted that the rise time during impulse coil test are shorter than in the case with 4 coils in parallel. This is due to the fact that the current supplied is lower and the tendency of SiC switch to produce faster dV/dt under low current, the applied electrical stress regarding turn insulation is thus higher. An example of PD acquisition can be seen in Fig 24.

But, as these results demonstrate, the PDIV difference between these two test is only 20Vpeak, within the error margin, and no large influence of the dV/dt between 5kV/µs and 10kV/µs could be observed on the turn to turn PDIV. This may be due to the fact that there are actually few turns per coil and a lot magnet wires (strands) in parallel per coil.

Table 20. Phase to ground AC Partial Discharge tests for stator n°3

| Impulse test on each coil of phase V (blue) | |
|---|---|
| Coil | PDIV |
| V1 | >1600 Vpeak |
| V2 | 1280 Vpeak [1203-1360]Vpeak with 95% confidence bounds<br><br>DC Bus : 780V<br>Overshot : 480V<br>Rise time : 120ns<br>dV/dt : 10.5kV/µs |
| V3 | >1600 Vpeak |
| V4 | >1600 Vpeak |

## Reduction of Electrical Stress

### *Preventing PD in Turn-to-Turn Insulation*

The critical area of insulation for phase V is the turn-to-turn insulation of coil 2 (named blue/yellow). It thus seems interesting to change the coil connection to try to reduce the electrical stress applied to it. The weakest coil V2 was connected in series to coil V4 which does not present turn-to-turn PD. (Fig. 25)

It can be seen in Fig. 26 that the electrical stress applied to the turn-to-turn critical area has been decreased because PD are no longer observed at coil V2 PDIV. This was expected since the DC bus voltage is now divided between the 2 coils in series instead of being applied to all 4 coils at the same time. Furthermore despite the increase of the DC bus up to 970VDC (Fig 27), no PD could be observed. Moreover, no large impulse propagation effect such as ringing or very uneven voltage distribution could be observed along the 2 coils, explaining why no PD could be observed at coil V2 PDIV.

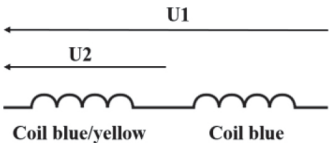


Figure 25. Serial configuration

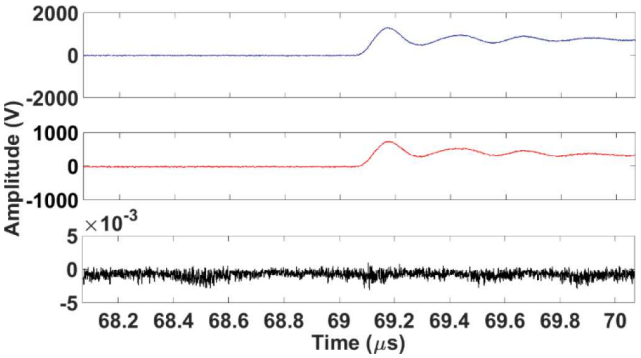


Figure 26. Two coils voltage U1 (blue) First coil voltage U2 (red) Sensor signal filtered at 200 MHz (black) at coil 2 PDIV (780 V DC bus)

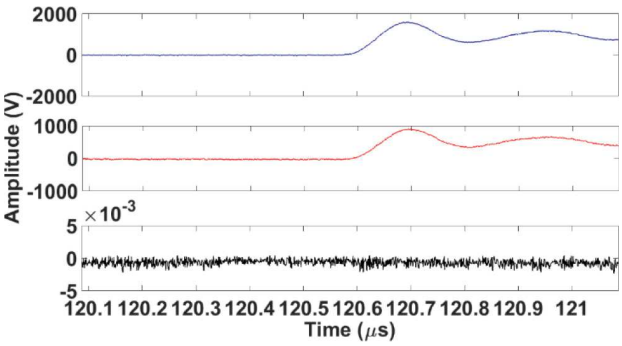


Figure 27. Two coils voltage U1 (blue) First coil voltage U2 (red) Sensor signal filtered at 200 MHz (black) at 970 V DCbus

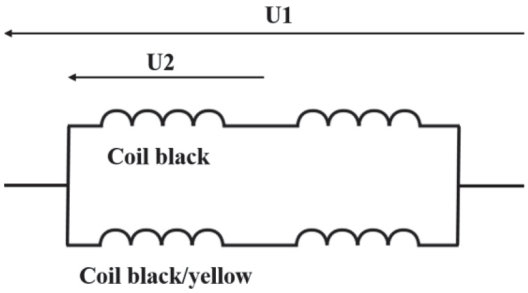


Figure 28. Serial/parallel configuration

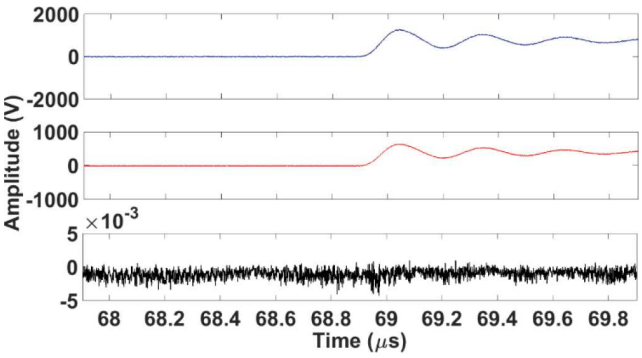


Figure 29. Phase voltage U1 (blue) First coil voltage of one parallel branch U2 (red) Sensor signal filtered at 200 MHz (black) at PDIV (385 V DCbus)

### *Preventing PD in Coil to Coil Insulation*

The critical insulation area for phase W has be identified to be coil-to-coil insulation between W1 (black yellow) and W4 (black).To mitigate the effect of this weakness, coil configuration 2 was chosen with 2 coils series in parallel. (Fig. 28)

We can see in Fig.29 that the electrical stress decreased because there is not any PD at the voltage previously observed. As before, voltage is now divided between coils in series which, in turn, reduce the coil to coil stress. DC Bus voltage has been increased up to 970VDC without observing any PD signals.

***Discussion about Winding Configuration Influence***

Using results from coil-to-coil and impulse tests, the advantage of configuration n°2 was demonstrated over nominal configuration 3 for the same insulation system. What could have been expected from a simple voltage distribution analysis on coils have been tested experimentally on a typical electric stator. This holds true for this particular winding configuration with concentric winding diagram segregating coils and coils of few turns which does not prevent significant sensitivity to fast impulse.

Although these conclusions could not be directly extended on any winding configuration, the same kind of analysis could lead to enhanced PDIV performance on other electric motor even without knowing *a priori* of all insulation in the motor. Obviously, this better PDIV performance come at a cost regarding electromechanical performance as shown by the qualitative tendencies about back EMF, torque and speed.

## Summary and Conclusions

This paper illustrates with stator n°2 the robustness of non-intrusive detection method at low pressure under SiC impulse voltage. Both analog filtering and wavelet analysis prove to be able to determine PDIV with a better signal to noise ratio for the latter.

The experimental set-up consisting in a three phases SiC inverter drive and a vacuum chamber is able to reproduce any PWM waveform on a wide range of electric stator both at atmospheric pressure and at low altitude. The 1000V DC bus is able to test electric stator with a large design margin compared with 540VDC aeronautic electric network. The failure of stator n°1 illustrates the destructive potential of non-detected partial discharge

This study showed how, without any knowledge of PDIV of each insulation within the electric motor, a safer winding configuration could be selected with a trade-off regarding electromechanical performance (back EMF, torque, speed). We recommend that motor designers take advantages of multiple winding configuration with similar insulation system and identical electromechanical performance to evaluate insulation performance

## Future Work and Improvements

As a conclusion of this technical report, further investigations will be performed.

- Study of different winding configuration for the same insulation system and analysis of electromechanical trade-off
- Impact of variable dV/dt on each phase PDIV
- Impact of temperature and low pressure on compressed end-winding
- Detailed study of electromagnetic noise function of dV/dt
- Development of an advanced three-phase wavelet numerical processing taking into account dV/dt value

## References


1. Cotton, A. Nelms and Husband M., "Higher voltage aircraft power systems," in IEEE Aerospace and Electronic Systems Magazine, vol. 23, no. 2, pp. 25-32, Feb. 2008. doi:10.1109/MAES.2008.4460728
2. Billard T., Lebey T., Fresnet F., “Partial discharge in electric motor fed by a PWM inverter: off-line and on-line detection," in Dielectrics and Electrical Insulation, IEEE Transactions on, vol.21, no.3, pp.1235-1242, June 2014. doi:10.1109/TDEI.2014.6832270
3. Cella B., Lebey T. and Abadie C., "Partial discharges measurements at the constituents' level of aerospace power electronics converters" Electrical Insulation Conference (EIC), 2015 IEEE, Seattle, WA, 2015, pp. 274-277. doi:10.1109/ICACACT.2014.7223587
4. Grosjean D. F., Schweickart D. L., Kasten D. G., Sebo S. A. and Liu X., "Development of procedures for partial discharge measurements at low pressures in air, argon and helium," in IEEE Transactions on Dielectrics and Electrical Insulation, vol. 15, no. 6, pp. 1535-1543, December 2008. doi:10.1109/TDEI.2008.4712655
5. Billard T., Lebey T., and Abadie C., “Recent advances in on-line Partial Discharge detection in electric power conversion chains used in aeronautics”, WEMDC17 Conference
6. Billard, T., Abadie, C., and Taghia, B., "Non-Intrusive Partial Discharges Investigations on Aeronautic Motors," SAE Technical Paper 2016-01-2058, 2016, doi:10.4271/2016-01-2058.
7. IEEE Guide for the Measurement of Partial Discharges in AC Electric Machinery - 2010
8. Bartnikas R. and McMahon E. J., “Engineering dielectrics - Volume 1 - Corona measurements and interpretation”, American Society for Testing and Materials - STP669, published in 1979
9. Roboam X., "New trends and challenges of electrical networks embedded in “more electrical aircraft”," Industrial Electronics (ISIE), 2011 IEEE International Symposium on, Gdansk, 2011, pp. 26-31. doi: 10.1109/ISIE.2011.5984130
10. Rosero J. A., Ortega J. A., Aldabas E. and Romeral L., "Moving towards a more electric aircraft," in IEEE Aerospace and Electronic Systems Magazine, vol. 22, no. 3, pp. 3-9, March 2007. doi: 10.1109/MAES.2007.340500
11. Karimi K.J., “Future Aircraft Power Systems - Integration Challenges”.2007
12. Moir I., Seabridge A. “Aircraft Systems: Mechanical, Electrical and Avionics Subsystems Integration, 3rd Edition”, August 2011
13. Rotating Electrical Machines - Part 18-41: Qualification and Type Tests for Type I - Electrical Insulation Systems Used in Rotating Electrical Machines Fed from Voltage Converters, IEC 60034-18-41 - TS Ed. 1.0, 2007
14. Dos Santos V., Cougo B., Roux N., Sareni B., Revol B., Carayon J.-P. (2017): Trade-off between Losses and EMI Issues in Three-Phase SiC Inverters for Aircraft Applications. EMC 2017, Aug. 7 - 11th, 2017, Washington (USA).

15. Vigneshwaran B., Maheswari R. V., and Subburaj P., “An improved threshold estimation technique for partial discharge signal denoising using Wavelet Transform,” in 2013 International Conference on Circuits, Power and Computing Technologies (ICCPCT), 2013, pp. 300-305.
16. Sharmila G., Maheswari R. V., and Subburaj P., “Partial discharge signal denoising using wavelet techniques-on site measurements,” in 2013 International Conference on Circuits, Power and Computing Technologies (I CCPCT), 2013, pp. 673-678.
17. Burrus C. S., Gopinath R. A., and Guo H., Introduction to Wavelets and Wavelet Transforms: A Primer, 1st ed. Upper Saddle River, N.J: Prentice Hall, 1997.
18. Zhang H., Blackburn T. R., Phung B. T., and Sen D., “A novel wavelet transform technique for on-line partial discharge measurements. 1. WT de-noising algorithm,” IEEE Trans. Dielectr. Electr. Insul., vol. 14, no. 1, pp. 3-14, Feb. 2007.
19. Seo J., Ma H., and Saha T., “Probabilistic wavelet transform for partial discharge measurement of transformer,” IEEE Trans. Dielectr. Electr. Insul., vol. 22, no. 2, pp. 1105-1117, Apr. 2015.
20. Altay O. and Kalenderli O., “Wavelet base selection for denoising and extraction of partial discharge pulses in noisy environment,” IET Sci. Meas. Technol., vol. 9, no. 3, pp. 276-284, 2015.
21. Abadie C., Billard T. and Lebey T., "Numerical signal processing methods for partial discharge detection in more electrical aircraft," 2016 IEEE International Conference on Dielectrics (ICD), Montpellier, 2016, pp. 540-543.

## Contact Information

Please direct contact to Dr. Thibaut Billard, research engineer and electromechanical designer at IRT Saint-Exupéry on temporary assignment from Liebherr Aerospace, Toulouse, France

Thibaut.billard@irt-saintexupery.com

## Acknowledgements

The information presented in this paper is the result of contributions from many team members of the more electrical aircraft - reliability and integration project. The authors would like to thank the following individuals for thoughtful discussions and input, Dr. Bernardo Cougo and Dr. Laurent Albert.

## Definitions/abbreviations

**AC** - Alternative Current

**DC** - Direct Current

**EIS** - Electrical Insulation System

**EMF** - Counter-electromotive force

**FFT** - Fast Fourier Transform

**IRT** - Institute of Technological Research

**MEA** - More Electrical Aircraft

**PD** - Partial discharge

**PDIV** - Partial Discharge Inception voltage

**PMSM** - Permanent Magnet Synchronous Motor

**PWM** - Pulse Width Modulation

**SiC** - Silicon Carbide

**SNR** - Signal to Noise Ratio

**WT** - Wavelet Transform